

MECHANISMS CONTROLLING Ca ION RELEASE FROM SOL-GEL DERIVED IN SITU APATITE-SILICA NANOCOMPOSITE POWDER

#SEYED MOHSEN LATIFI* **, MOHAMMADHOSSEIN FATHI* ***,
JALEH VARSHOSAZ** , NILOUFAR GHOCHAGHI****

*Biomaterials Research Group, Department of Materials Engineering,
Isfahan University of Technology, Isfahan 84156-83111, Iran

**Department of Pharmaceutics, Faculty of Pharmacy and Novel Drug Delivery Systems Research Centre,
Isfahan University of Medical Sciences, PO Box 81745-359, Isfahan, Iran

***Dental Materials Research Center, Isfahan University of Medical Sciences, Isfahan, Iran

****Department of Biomedical Engineering, Virginia Commonwealth University, Richmond, Virginia, 23284, USA

#E-mail: sm.latifi@ma.iut.ac.ir

Submitted January 15, 2015; accepted April 17, 2015

Keywords: Ca ion, Silica, Apatite, Nanocomposite powder, Sol-gel

Ca ion release from bioactive biomaterials could play an important role in their bioactivity and osteoconductivity properties. In order to improve hydroxyapatite (HA) dissolution rate, in situ apatite-silica nanocomposite powders with various silica contents were synthesized via sol-gel method and mechanisms controlling the Ca ion release from them were investigated. Obtained powders were characterized by X-ray diffraction (XRD) and transmission electron spectroscopy (TEM) techniques, acid dissolution test, and spectroscopy by atomic absorption spectrometer (AAS). Results indicated the possible incorporation of SiO_4^{4-} into the HA structure and tendency of amorphous silica to cover the surface of HA particles. However, 20 wt. % silica was the lowest amount that fully covered HA particles. All of the nanocomposite powders showed more Ca ion release compared with pure HA, and HA - 10 wt. % silica had the highest Ca ion release. The crystallinity, the crystallite size, and the content of HA, along with the integrity, thickness, and ion diffusion possibility through the amorphous silica layer on the surface of HA, were factors that varied due to changes in the silica content and were affected the Ca ion release from nanocomposite powders.

INTRODUCTION

Bone diseases and defects are serious issues that affect the patients' quality of life [1]. Bioceramics as synthetic bone graft substitute materials are an appropriate medical intervention due to availability, reproducibility, and reliability [2-3]. The aim of the bone graft, besides restoration of the bone defect, is to support the repaired area by inducing new bone ingrowth into the defect site [4].

Synthetic hydroxyapatite ($\text{Ca}_{10}(\text{PO}_4)_6(\text{OH})_2$; HA) consists of the majority of the inorganic elements of human bones and teeth. HA is one of the most important candidates for bone graft substitute materials due to its biocompatibility, bioactivity, and osteoconductivity [5-7]. However, very slow dissolution rate is one of disadvantage of the synthetic stoichiometric HA that could interfere with the growth of new bone tissue [8-10]. Moreover, slow dissolution rate of HA limits its bioactivity and leads to low reactivity of HA with existing bone [11-12].

It has been reported that the bioactivity and the osteoconductivity properties of HA are related to its dissolution behavior in human body environment [13-

15]. In other words, the dissolution of calcium and phosphate ions from the HA may occur by means of the surrounding environment (extracellular fluid) and may also be actively mediated by osteoclast cells [16]. The HA dissolution lead to an increase in the concentrations of calcium and inorganic phosphate in the gap between the existing bone and the HA graft [17], and would enhance the formation of new natural bone by consuming these ions [13-14]. In this case, Ca ions have a key role in HA initial nucleation. In fact, the heterogeneous nucleation of HA is accelerated by the accumulation of Ca ions caused by the attractive interaction between the Ca ions and the negatively charged surface [18]. The HA precipitated into this gap will ensure integration of the HA graft with the existing bone. So, the accelerating this process could make a significant improvement in the bioactivity of HA and also in the quality of life of the patient [19].

Silicon plays an important role in bone metabolism [20]. It is also vital to the growth and development of biological tissue such as bone and teeth [21]. It was reported that the substitution of SiO_4^{4-} in the HA structure increase its solubility [19, 22-23]. Also, the formation of an amorphous silica layer on the surface of HA could change the HA dissolution [24].

Based on the importance of enhancing a HA graft's bonding to bone and the vital role of Ca ions in this process, the main objective of this study was to improve HA dissolution by means of silica and to determine the mechanisms controlling the Ca ion release from HA-silica nanocomposite powders.

EXPERIMENTAL

Preparation of apatite-silica nanocomposite powders

Apatite-silica nanocomposite powders were prepared by optimized methodology described in our previous research [25]. Calcium nitrate tetrahydrate [$\text{Ca}(\text{NO}_3)_2 \cdot 4\text{H}_2\text{O}$, Merck] and phosphoric pentoxide [P_2O_5 , Merck] were dissolved in separate beakers containing absolute ethanol [$\text{C}_2\text{H}_5\text{OH}$, Merck]. Both solutions were mixed at a Ca/P molar ratio of 5:3, and the mixture was stirred for ~3 h at 30°C and was then aged for ~6 h at 30°C. Different amounts of tetraethylorthosilicate (TEOS) [$\text{Si}(\text{OC}_2\text{H}_5)_4$, Merck] were added drop wise to the aged solutions of HA under continuous stirring. After ~1 h of stirring, 0.1 N HNO_3 and acetic acid were added as the catalyst. The molar ratio of $\text{H}_2\text{O}/\text{TEOS}$ and water/acetic acid was 2:1 and 7:1, respectively. Final mixtures were stirred for ~3 h at 30°C and were then aged for 24 h at room temperature under static conditions. The resulting gels were then dried at 80°C for 24 h. The dry powders were crushed using a ball mill (Fretch Pulverisette 5) with a 125 ml zirconia vial and four 20 mm diameter zirconia balls at room temperature. The process was performed with a ball/powder mass ratio of 20:1 and a rotation speed of 150 rpm for 90 min. They were calcinated by heating to 600°C at 5°C·min⁻¹, kept at the mentioned temperature for 30 min, and then cooled to room temperature. The obtained nanocomposite powders were referred to as HA-5S, HA-10S, HA-20S, etc., corresponding to the calculated content of silica (wt. %) in the nanocomposite powders. For comparison purposes, pure HA nanopowder was also prepared.

Characterization of nanocomposite powders

Phase structure and crystallinity of the prepared powders were analyzed and determined by an X-ray diffractometer (XRD, Philips X'Pert-MPD) using a Cu K_α radiation ($\lambda = 0.15418$ nm, 40 kV and 30 mA) over the range of 10 - 70° with a step size of 0.05°·s⁻¹. Lattice parameters (a and c) and unit cell volume of the prepared powders were calculated using the obtained XRD patterns and the cell parameters refinement software, Celref V.3. [26].

Transmission electron microscopy (TEM, Philips CM120) was used to study and determine the morphology and the particle size of the powders.

An acid dissolution test was carried out by dispersing the powder samples with a ratio of 8 mg·ml⁻¹ in 2M HCl. After 30 min in an ultrasonic bath, the apparent color of the solutions/suspensions was observed.

A physiological saline solution (0.9 wt. % NaCl) was used to evaluate the dissolution behavior of the powders. For this purpose, vials containing the prepared powder samples and the physiological saline solution at a ratio of 1mg·ml⁻¹ were placed in a shaking water bath at 37°C and 50 rpm. After 6 h, the dissolution of calcium ions in the filtered physiological saline solution was determined by an atomic absorption spectrometer (AAS, Perkin-Elmer 2380).

RESULTS AND DISCUSSION

X-ray diffraction analysis

Figure 1 shows the XRD patterns of the prepared apatite-silica nanocomposite powders accompanying by HA nanopowder for comparison. Whereas silica is an amorphous phase, no peak related to silica was recorded in the XRD patterns. However, the presence of silica by its effect on the XRD patterns has become quite visible.

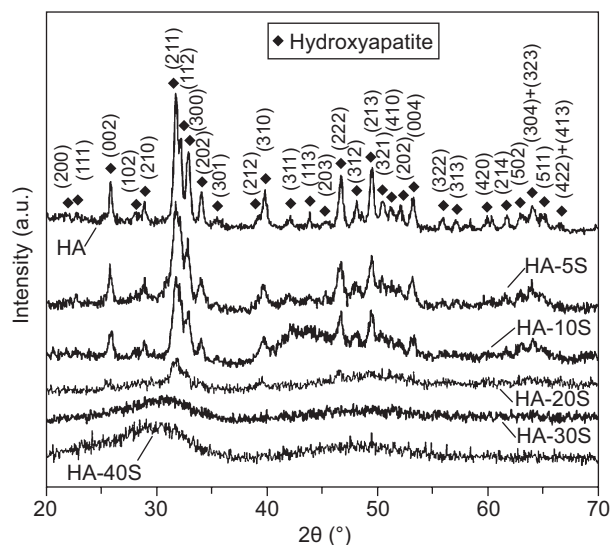


Figure 1. XRD patterns of the prepared HA nanopowder and apatite-silica nanocomposite powders with different amounts of silica.

The lattice parameters and the unit cell volume of pure HA along with HA in HA-5S and HA-10S nanocomposite powders, calculated by the Celref soft-ware using XRD diffraction data, are presented in Table 1. It should be noted that the calculation of the lattice parameters of HA in other nanocomposite powders was difficult due to the very low intensity of the HA peaks. Therefore, it is not presented in Table 1. In agreement with other researchers [27-28], the higher unit cell volumes of HA in nanocomposite powders rather than HA are related to the incorporation of SiO_4^{4-} into the

HA structure. Also, the higher unit cell volume of HA in HA-10S nanocomposite powder rather than HA-5S can be attributed to the higher incorporation of SiO_4^{4-} into the HA structure. The incorporation of SiO_4^{4-} into the HA structure reduces to some extent the crystallinity of HA [22].

Table 1. Lattice parameters (a and c) and unit cell volume of HA, HA-5S and HA-10S nanocomposite powders.

Compound	a-Axis (Å)	c-Axis (Å)	Unit cell volume (Å ³)
HA	9.4093	6.8862	527.98
HA-5S	9.4329	6.8794	530.12
HA-10S	9.4345	6.8905	531.16

Due to the limited incorporation of SiO_4^{4-} into the HA structure [27], the intense change in the XRD patterns of HA-20S to HA-40S nanocomposite powders is related to the special configuration of the amorphous silica phase and the HA phase in these nanocomposite powders. In other words, as the large portion of HA-20S nanocomposite powder is composed of the HA phase, it was expected that its XRD pattern would represent obvious peaks with high intensity indicative of the HA phase. However, contrasting to expectation, the HA peaks have very low intensity. In fact, the silica amorphous phase in nanocomposite powders covered the surface of HA [24, 29-30], acting as a barrier for the recognition of HA by an X-ray beam. Therefore, the existence of the HA phase, which composes a large portion of HA-20S nanocomposite powder, shows a lower level on the X-ray diffraction than its actual level. The higher the silica content is in the nanocomposite powder, the higher the thickness of the amorphous silica layer on the surface of HA [24, 29]. Consequently, this fact is intensified more in HA-30S and HA-40S nanocomposite powders.

It is worth mentioning that the silica layer on the surface of HA not only acts as a barrier for recognition

of HA by an X-ray beam but can also act as a hindrance against crystallization of the HA phase and has a reduction effect on the crystallinity of HA to some extent by limiting its atomic arrangement [24].

Acid dissolution test

Figure 2 shows the effect of an acidic environment (2 M HCl solution) on nanocomposite powders compared with HA powder. Hydroxyapatite's reaction ability in an acidic environment (below pH 4.8) leads to HA dissolution [30-32], which causes a change in the color of the solution. However, silica is resistant to an acidic environment, as it does not change the color of its solution [30]. Considering the different behaviors of HA and silica in acidic environments, acid dissolution test can be indicative of the configuration of amorphous silica phase in nanocomposite powders. Additionally, it can be indicative of the qualitative efficiency of surface modification of HA with a silica amorphous layer.

As shown in Figure 2, HA-5S nanocomposite powder has the same color as HA in the acidic environment. This matter is indicative of the insufficiency of silica content to cover the surface of HA. However, by increasing the silica content to 10 wt. % and higher, the ability of silica for covering the surface of HA considerably increases and the color of the acidic environments approach each other due to the distribution of nanocomposite powders in them. Covering the surface of HA with the amorphous silica layer for HA-10S to HA-40S nanocomposite powders is desirable, but a near full covering of HA for HA-20S to HA-40S nanocomposite powders protected the HA core against the acidic environment. A faint color differential, which is visible in the acidic environments containing HA-10S to HA-40S nanocomposite powders, can be attributed to the integrity [30], thickness [24, 29], and nature of the silica layer on the surface of HA [30]. This matter is more evidenced in nanocomposite powders with lower silica content, especially in HA-10S nanocomposite

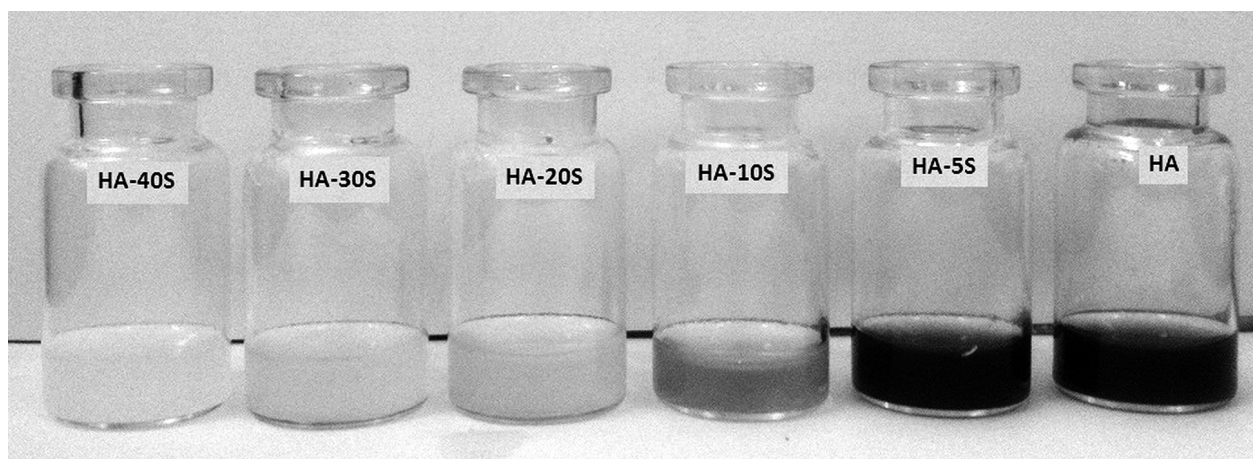
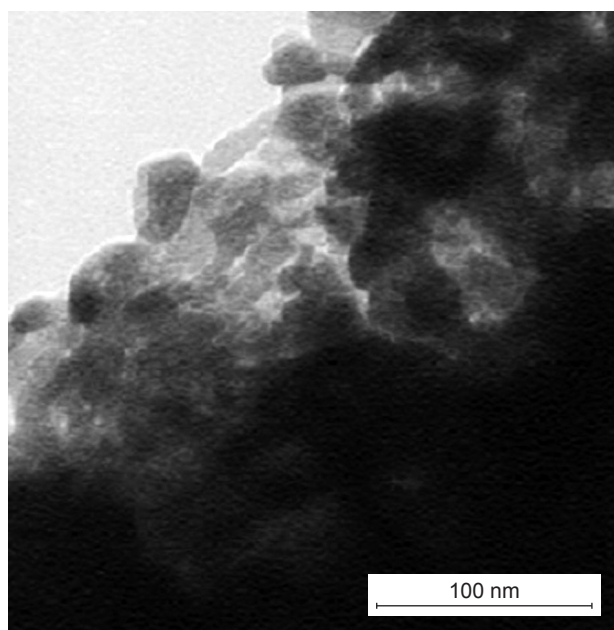
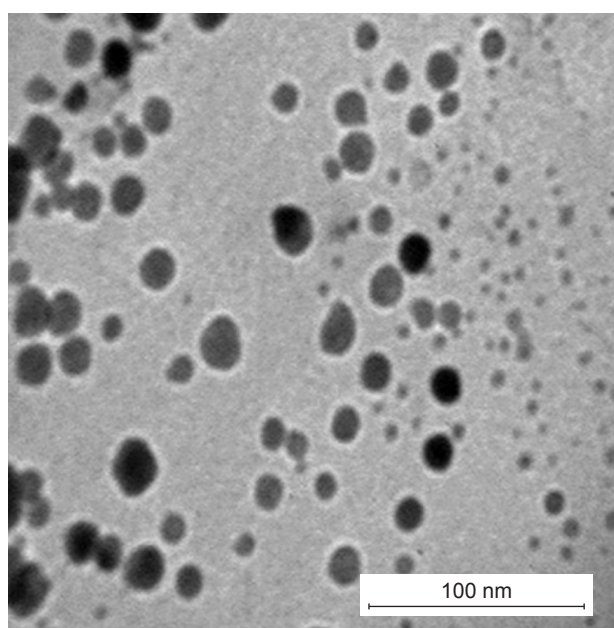


Figure 2. Acid dissolution test of HA nanopowder, and apatite-silica nanocomposite powder samples in 2 M HCl solution.

powder. In other words, the darker color of the acidic environment containing HA-10S nanocomposite powder can be a consequence of the low integrity in the silica layer on the surface of HA. Moreover, the amorphous silica layer on the surface of HA has the potential to act as a semi-permeable layer with a selective diffusive Ca ion property [30]. So, the lower the silica content in nanocomposite powders, the lower the thickness of amorphous silica layer on the surface of HA, facilitating selective and controlled ion diffusion.



a) HA-5S



b) HA-40S

Figure 3. TEM images of HA-5S (a) and HA-40S (b) nanocomposite powders.

TEM analysis

Figure 3 shows the TEM images of HA-5S and HA-40S nanocomposite powders. The particles related to HA-5S nanocomposite powders have an elongated shape with a size of about 30nm in the longest dimension, but the particles related to HA-40S nanocomposite powders have an orbicular appearance with a size of about 15 nm. The significant changes in the morphology and the size of particles can be attributed to the silica layer. In fact, the growth of HA crystallite is restricted due to the presence of the silica layer on the surface of HA during the ageing process [24, 29].

Dissolution behavior

Figure 4 shows the degree of Ca ion release in physiological saline solution for HA and various compounds of apatite-silica nanocomposite powders based on the same magnitude powder (Figure 4a) and the same HA magnitude (Figure 4b). In other words, the HA content is decreased by increasing the silica content in nano-composite powders. Therefore, Figure 4b was extracted from Figure 4a based on the same HA content in nanocomposite powders. Considering that the objective of conducting this test was solely to study the dissolution behavior of nanocomposite powders, a 6 hour period was used in order to avoid disorder in the evaluation of results due to the reprecipitation of ions.

The overall study of Figure 4a indicates that all nanocomposite powders in comparison with pure HA have more Ca ion release and among them, HA-10S nanocomposite powder has the highest. It should be noted that all powders have the same magnitude, with nanocomposite powders having a lower amount of HA in comparison with pure HA, and this difference is intensified with increasing the silica content. Moreover, according to the results of the acid dissolution test, a full covering of HA by silica is developed for HA-20S to HA-40S nanocomposite powders. So, the higher level Ca ion release from HA-20S to HA-40S nanocomposite powders compared with pure HA can prove the diffusion possibility of Ca ion from an amorphous silica layer on the surface of HA [30].

According to literature, the incorporation of SiO_4^{4-} into the HA structure reduces the crystallinity [22] and the crystallite size of HA [23, 33], which lead to increase the solubility of HA [19, 22-23, 33]. So, the increase in Ca ion release for HA-5S nanocomposite powder compared to pure HA is the consequence of silica's effect on the HA structure. In fact, the incorporation of SiO_4^{4-} into the HA structure and also the hindering effect of a silica layer against HA crystallization lead to a reduction in the crystallinity and the crystallite size of HA. Consequently, accumulation of these factors leads to increased Ca ion release from HA-5S nanocomposite powder.

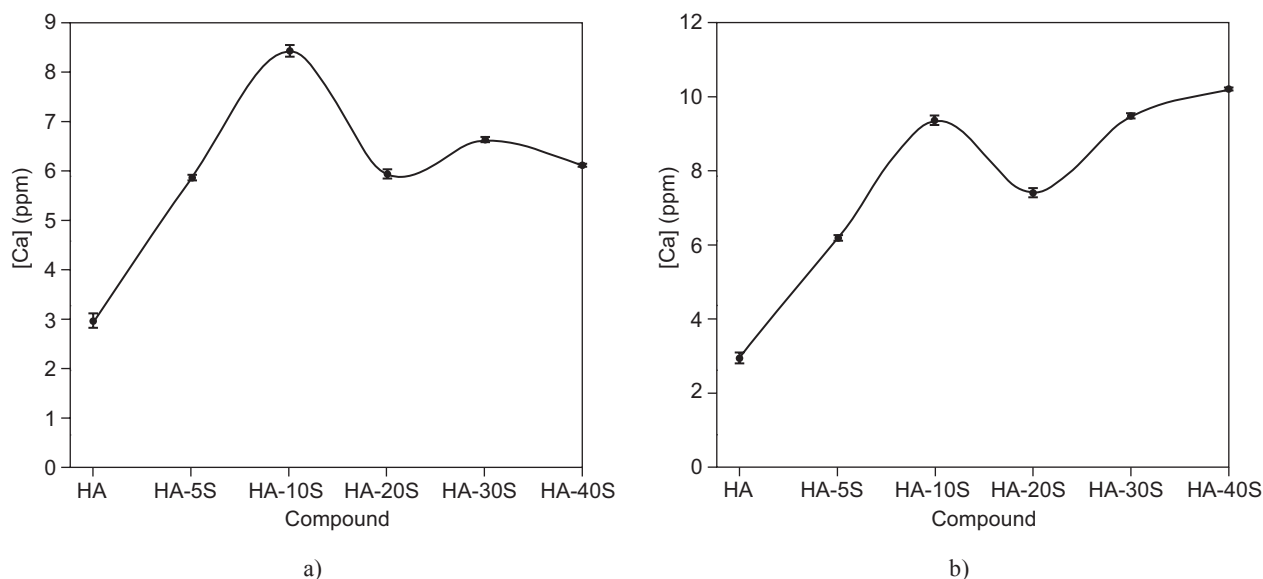


Figure 4. Ca ion release in physiological saline solution for HA nanopowder and apatite-silica nanocomposite powders after 6 h at 37°C and 50 rpm based on the same magnitude powder (a), and the same HA magnitude, which derived of figure 4a (b).

By increasing silica content to 10 wt. % in HA-10S nanocomposite powder, the incorporation of SiO_4^{4-} into the HA structure and the hindering effect of silica layer against crystallization of HA would be further increased, causing to more reduction in the crystallinity and the crystallite size of HA. Moreover, considering the results of the acid dissolution test, the barrier effect of the silica layer on the surface of HA to Ca ion release is low due to the low integrity and the small thickness of this layer in HA-10S nanocomposite powder. So, the foregoing factors lead to an increase in Ca ion release from HA-10S nanocomposite powder compared to HA-5S nanocomposite powder.

Reduction in the Ca ion release level from HA-20S nanocomposite powder compared to HA-10S nanocomposite powder can be attributed to the full covering of HA with the silica layer, which is in good agreement with result of the acid dissolution test. In fact, the silica protective layer on the surface of HA acts as an obstacle for Ca ion release and suppresses the impact of the hindering effect of the silica layer against crystallization of HA, which lead to a decrease in Ca ion release from HA.

Considering the results of the acid dissolution test, full covering of HA is developed by silica for HA-20S to HA-40S nanocomposite powders. So, the higher Ca ion release from HA-30S nanocomposite powder compared to HA-20S nanocomposite powder can be attributed to the dominance of the hindering effect of the silica layer against HA crystallization that compensates for the impact of the silica protective layer on the surface of HA that acts as an obstacle for Ca ion release. The results shown in Figure 4b for HA-20S to HA-30S nanocomposite powders confirms the foregoing reasoning.

HA-40S nanocomposite powder in comparison with HA-30S nanocomposite powder has lower Ca ion release. This matter can be attributed to a decrease of HA content on one hand and to an increase of the thickness of the silica layer on the surface of HA on the other hand. The foregoing reasoning is in agreement with the result of Figure 4b for HA-30S to HA-40S nanocomposite powders. In fact, the decreasing slope of dashed line in Figure 4b for HA-20S to HA-40S nanocomposite powders indicates the increasing thickness of the silica layer on the surface of HA.

CONCLUSIONS

The results of this study demonstrated the incorporation of SiO_4^{4-} into the HA structure and the tendency of the amorphous silica for covering the surface of HA particles in Sol-gel derived in situ apatite-silica nanocomposite powders, but the full covering of HA was developed by amorphous silica layer for HA-20S to HA-40S nanocomposite powders. Also, increasing the silica content in the nanocomposite powders showed a reduction effect on particle size of powders and changed their morphology. All of the nanocomposite powders compared with pure HA had more Ca ion release. However, HA-10S nanocomposite powder had the highest Ca ion release. The Ca ion release from nanocomposite powders was determined by the competition between three processes: 1) the reduction in the crystallinity and the crystallite size of HA due to the hindering effect of the silica layer on the surface of HA against HA crystallization and the incorporation of SiO_4^{4-} into the HA structure, 2) the selective diffusion

of Ca ions through the silica layer, and 3) the reduction in the HA content and the increase of thickness and integrity of the silica layer on the surface of HA. The first and second processes had a positive effect and the third process had a negative effect on the Ca ion release from nanocomposite powders. The variation of the silica content in nanocomposite powders lead to changes in the impact of the above-mentioned processes and, consequently, the Ca ion release from them would be affected.

Acknowledgment

The authors are grateful for the support to this research by the Isfahan University of Technology and Isfahan University of Medical Sciences.

REFERENCES

1. Hench L.L.: *J. Am. Ceram. Soc.* **74**, 1487 (1991).
2. Ranter B.D., Hoffman A.S., Schoen F.J., Lemons J.E.: *Biomaterials science. An Introduction to Materials in Medicine*, p. 484, 1996.
3. Eshtiagh-Hosseini H., Housaindokht M. R., Chahkandi M.: *Mater. Chem. Phys.* **106**, 310 (2007).
4. Goulet J. A., Senunas L.E., DeSilva G.L., Greenfield M.L.: *Clin. Orthop. Relat. Res.* **339**, 76 (1997).
5. Vallet-Regi M.: *J. Chem. Soc. Dalton Trans.* **2**, 97 (2001).
6. Kokubo T., Kim H. M., Kawashita M.: *Biomaterials* **24**, 2161 (2003).
7. Shirkhazadeh M.: *J. Mater. Sci. Mater. Med.* **16**, 37 (2005).
8. Jongwattanapisan P., Charoenphandhu N., Krishnamra N., Thongbunchoo J., Tang I., Hoonsawat R., Meejoo Smith S., Pon-On W.: *Mater. Sci. Eng. C* **31**, 290 (2011).
9. David E., Derek M., Mauro A.: *Soft. Matter* **5**, 938 (2009).
10. Narayan B., Zhensheng L., Jonathan G., Matthew L., Ashleigh C., Dennis E., Omid V., Ming-Hong C., Yong Z., Richard G.E., Migin Z.: *Adv. Mater.* **21**, 2792 (2009).
11. Ducheyne P., Radin S., King L.: *J. Biomed. Mater. Res.* **27**, 25 (1993).
12. Mastrogiacoma M., Muraglia A., Komlev V., Peryin F., Rus-tichelli F., Crovace A., Cancedda R.: *Orthod. Craniofacial. Res.* **8**, 277 (2005).
13. Gledhill H.C., Turner I.G., Doyle C.: *Biomaterials* **22**, 695 (2001).
14. Cleries L., Fernandez-Pradas J.M., Sardin G., Morenza J.L.: *Biomaterials* **19**, 1483 (1998).
15. Weng J., Liu Q., Wolke J.G.C., Zhang X., de Groot K.: *Biomaterials* **18**, 1027 (1995).
16. Doi Y., Shibutani T., Moriwake Y., Kajimoto T., Iwayama Y.: *J. Biomed. Mater. Res.* **39**, 603 (1997).
17. Amarh-Bouali S., Rey C., Lebugle A., Bernache D.: *Biomaterials* **15**, 269 (1994).
18. Zhu P.X., Masuda Y., Koumoto K.: *J. Colloid. Interface. Sci.* **243**, 31 (2001).
19. Porter A.E., Patel N., Skepper J.N., Best S.M., Bonfield W.: *Biomaterials* **24**, 4609 (2003).
20. Carlisle E.M.: *J. Nutr.* **106**, 478 (1976).
21. Carlisle E.M.: *Calcif. Tissue. Int.* **33**, 27 (1981).
22. Boanini E., Gazzano M., Bigi A.: *Acta. Biomater.* **6**, 1882 (2010).
23. Bang L. T., Long B. D., Othman R.: *The. Sci. World. J.* **2014**, 1 (2014).
24. Latifi S. M., Fathi M. H., Golozar M. A.: *Adv. Appl. Ceram.* **110**, 8 (2011).
25. Latifi S. M., Fathi M. H., Varshosaz J.: *Ceram. Int.* **41**, 9476 (2015).
26. Ahmadi T., Monshi A., Mortazavi V., Fathi M. H., Sharifi S., Hashemi Beni B., Moghare Abed A., Kheradmandfard M., Sharifnabi A.: *Ceram. Int.* **40**, 8341 (2014).
27. Palard M., Champion E.: *J. Solid State Chem.* **181**, 1950 (2008).
28. Kim S.R., Lee J.H., Kim Y.T., Riu D.H., Jung S.J., Lee Y.J., Chung S.C., Kim Y.H.: *Biomaterials* **24**, 1389 (2003).
29. Andersson J., Areva S., Spliethoff B., Lindén M.: *Biomaterials* **26**, 6827 (2005).
30. Borum L., Wilson Jr O.C.: *Biomaterials* **24**, 3681 (2003).
31. Brown P.W.: *J. Am. Ceram. Soc.* **75**, 17 (1992).
32. Vereecke G., Lemaître J.: *J. Cryst. Growth.* **104**, 820 (1990).
33. Ibrahim D. M., Mostafa A.A., Korowash S. I.: *Chem. Cent. J.* **74**, 2 (2011).